Electrochemistry and Spectral Characterization of Oxidized and Reduced ($TPPBr_x$)FeCl Where $TPPBr_x$ Is the Dianion of β-Brominated-Pyrrole Tetraphenylporphyrin and x Varies from 0 to 8

Pietro Tagliatesta,*,† Jun Li,‡ Marie Autret,‡ Eric Van Caemelbecke,‡ Anne Villard,‡ Francis D'Souza,§ and Karl M. Kadish*,‡

Dipartimento di Scienze e Tecnologie Chimiche, II Università degli Studi di Roma, 00133 Roma, Italy, Department of Chemistry, University of Houston, Houston, Texas 77204-5641, and Department of Chemistry, Wichita State University, 1845 Fairmont, Wichita, Kansas 67260-0051

Received February 8, 1996[⊗]

The electrochemistry and spectroelectrochemistry of ($TPPBr_x$)FeCl ($TPPBr_x$ is the dianion of β-brominated-pyrrole tetraphenylporphyrin and $x = 0-8$) were examined in PhCN containing tetra-*n*-butylammonium perchlorate (TBAP) as supporting electrolyte. Each compound undergoes two reversible to quasireversible one-electron oxidations and either three or four reductions within the potential limits of the solvent. The two oxidations occur at the conjugated porphyrin π ring system, and $\Delta E_{1/2}$ between these two electrode reactions increases as the molecule becomes more distorted. The overall reduction of each compound involves the stepwise electrogeneration *o*f an iron(II), iron(I), and iron(I) π anion radical. An equilibrium between chloride-bound and chloride-free iron(II) forms of the porphyrin is observed with association of the anionic ligand being favored for compounds with $x > 5$. Singly reduced ($TPPBr_x$)FeCl ($x = 0$ to $x = 6$) forms both mono- and bis-CO adducts in CH_2Cl_2. Only the mono-CO adduct is observed for ($TPPBr_7$)FeCl, and there is no binding at all of CO to ($TPPBr_8$)FeCl. The ν_{CO} of both the mono- and bis-adducts increases with increase in the number of Br groups, but in a nonlinear fashion which is explained in terms of two competing effects. One is the electron-withdrawing affinity of the Br substitutents and the other the nonplanarity of the macrocycle.

Introduction

Metallotetraphenylporphyrins bearing halogen substituents on the pyrrole β-positions of the macrocycle are of great interest since they show a high catalytic efficiency for the oxidation of organic substrates.[1−18] In the case of synthetic iron derivatives, this catalytic efficiency has been attributed to the presence of electron-withdrawing substituents on the macrocycle which makes the porphyrin π ring system harder to oxidize, thus stabilizing it against oxidative degradation.

The redox potentials of halogenated metalloporphyrins have, in several cases, been related to their catalytic efficiency[19] or the planarity of the molecules,[20−24] and with this in mind, our laboratory has examined the electrochemistry of ($TPPBr_x$)M where $TPPBr_x$ = the dianion of β-brominated-pyrrole tetraphenylporphyrin and M = Fe ($x = 0-8$)[24] or Co ($x = 0$, 6, 7, 8).[25] We now provide further details on the synthesis of the above series of brominated iron porphyrins, examine the binding of carbon monoxide by the Fe(II) forms of the porphyrins, and also report their full electrochemical and spectroelectrochemical characterization.

(TPP)FeCl (TPP = the dianion of tetraphenylporphyrin) undergoes three one-electron reductions and two one-electron oxidations in most nonaqueous solvents.[26] The first two reductions are metal-centered and involve a stepwise conversion of Fe(III) to Fe(II) followed by an Fe(II)/Fe(I) reaction at more negative potentials. The third reduction involves the porphyrin

† II Università degli Studi di Roma.
‡ University of Houston.
§ Wichita State University.
⊗ Abstract published in *Advance ACS Abstracts,* June 1, 1996.

(1) Lyons, J. E.; Ellis, P. E. *Metalloporphyrins in Catalytic Oxidations*; Dekker M.: New York, 1994; pp 297−324.
(2) Mansuy, D. *The Activation of Dioxygen and Homogeneous Catalytic Oxidation*; Plenum Press: New York and London, 1993; pp 347−358.
(3) Traylor, T. G.; Tsuchiya, S. *Inorg. Chem.* **1987**, *26*, 1338.
(4) Ellis, P. E.; Lyons, J. E. *Catal. Lett.* **1989**, *3*, 389.
(5) Meunier, B. *Chem. Rev.* **1992**, *92*, 1411.
(6) Ostovic, D.; Bruice, T. C. *Acc. Chem. Res.* **1992**, *25*, 314.
(7) Grinstaff, M. W.; Hill, M. G.; Labinger, J. A.; Gray, H. B. *Science* **1994**, *264*, 1311.
(8) Ellis, P. E.; Lyons, J. E. *J. Chem. Soc., Chem. Commun.* **1989**, 1315.
(9) Ellis, P. E.; Lyons, J. E. *Coord. Chem. Rev.* **1990**, *105*, 181.
(10) Lyons, J. E.; Ellis, P. E. *Catal. Lett.* **1991**, *8*, 45.
(11) Tsuchiya, S.; Seno, M. *Chem. Lett.* **1989**, *263*, 263.
(12) Hoffman, P.; Labat, G.; Robert, A.; Meunier, B. *Tetrahedron* **1990**, *31*, 1991.
(13) Wijesekera, T.; Matsumoto, A.; Dolphin, D.; Lexa, D. *Angew. Chem.* **1990**, *102*, 1073.
(14) Bartoli, J. F.; Brigaud, O.; Battioni, P.; Mansuy, D. *J. Chem. Soc., Chem. Commun.* **1991**, 440.
(15) Gonsalves, A. M.; Johnstone, R. A. W.; Pereira, M. M.; Shaw, J.; Sobral, J. F. *Tetrahedron Lett.* **1991**, *32*, 1355.
(16) Battioni, P.; Brigaud, O.; Desveaux, H.; Mansuy, D.; Traylor, T. G. *Tetrahedron. Lett.* **1991**, *32*, 2893.
(17) Bruice, T. C. *Mechanistic Principles of Enzyme Activity*; VCH Publishers: New York, 1988; Chapter 8.
(18) Traylor, T. G. *Tetrahedron Lett.* **1991**, *32*, 2893.
(19) Lyons, J. E.; Ellis, P. E., Jr. In *Metalloporphyrins in Catalytic Oxidations*; Sheldon, R. A., Ed.; Marcel Dekker Inc.; New York, 1994, p 314.
(20) Birnbaum, E. R.; Schaefer, W. P.; Labinger, J.-A.; Bercaw, J. E.; Gray, H. B. *Inorg. Chem.* **1995**, *34*, 1751.
(21) Grinstaff, M. W.; Hill, M. G.; Birnbaum, E. R.; Schaefer, W. P.; Labinger, J.-A.; Gray, H. B. *Inorg. Chem.* **1995**, *34*, 4896.
(22) Bhyrappa, P.; Krishnan, V. *Inorg. Chem.* **1991**, *30*, 239.
(23) Takeuchi, T.; Gray, H. B.; Goddard, W. A., III. *J. Am. Chem. Soc.* **1994**, *116*, 9730.
(24) Kadish, K. M.; D'Souza, F.; Villard, A.; Autret, M.; Van Caemelbecke, E.; Bianco, P.; Antonini, A.; Tagliatesta, P. *Inorg. Chem.* **1994**, *33*, 5169.
(25) D'Souza, F.; Villard, A.; Van Caemelbecke, E.; Franzen, M.; Boschi, T.; Tagliatesta, P.; Kadish, K. M. *Inorg. Chem.* **1993**, *32*, 4042.
(26) Kadish, K. M. *Prog. Inorg. Chem.* **1986**, *34*, 435.

S0020-1669(96)00148-6 CCC: $12.00

π ring system and leads to an Fe(I) π anion radical as a final reduction product, although a formal Fe(0) species has also been proposed for electrogenerated $[(TPP)Fe]^{2-}$.[27] The electroreduction of each $(TPPBr_x)FeCl$ complex also occurs *via* the stepwise electrogeneration of an iron(II), iron(I), and iron(I) π anion radical, but as will be shown, the number of electrode processes, as well as their half-wave or peak potentials, depend directly on the number of Br groups on the macrocycle.

Theoretical calculations[23,28,29] predict that the HOMO of porphyrins is more affected by the nonplanarity of the molecule than the LUMO, and this has been verified experimentally.[13,22,23,30−33] In addition, the $E_{1/2}$ for the first reversible oxidation of highly halogenated porphyrins does not vary linearly with increase in number of halogen groups. This deviation from linear free energy relationships has been quantitated in the case of $(TPPBr_x)FeCl$ where x varied from 0 to 8.[24]

The oxidation of $(TFPPX_8)Zn$ ($TFPPX_8$ = the dianion of tetrakis(pentafluorophenyl)porphyrin and X = Cl, Br, or CH_3) has also been reported in the literature.[34] The three nonplanar porphyrins are all oxidized at the macrocycle *via* two overlapping one-electron transfers[34] rather than *via* two well-separated one-electron steps as is the case for virtually all metalloporphyrins,[26] including (TPP)Zn and (OEP)Zn[26] (OEP = the dianion of octaethylporphyrin), both of which are planar. The two ring-centered oxidations of nonplanar $[(TPPBr_x)Co^{III}]^+$ (x = 6−8) are almost overlapped in PhCN,[25] and this can be compared to the case of $[(TPP)Co^{III}]^+$, a planar molecule which undergoes two well-separated one-electron oxidations at the macrocycle under the same solution conditions. This result suggests that there is a relationship between the $\Delta E_{1/2}$ separating the two ring-centered oxidations of a given cobalt or zinc metalloporphyrin and the planarity of the macrocycle. However, the same effect on $E_{1/2}$ is not observed for all metalloporphyrins, since the potential separation between the two oxidations (460 mV)[30] of nonplanar (OETPP)FeCl (OETPP = the dianion of octaethyltetraphenylporphyrin) is larger than $\Delta E_{1/2}$ between the two oxidations of (TPP)FeCl,[35] which is a planar molecule and has a $\Delta E_{1/2}$ of 260 mV under the same experimental conditions. It was therefore of interest to examine whether an increase or decrease of $\Delta E_{1/2}$ would be observed between the two oxidations of $(TPPBr_x)FeCl$ as the number of Br groups on the macrocycle was systematically increased from $x = 0$ to $x = 8$. It was also of interest to know how the presence of bulky electron-withdrawing substituents (and the resulting nonplanarity of the porphyrin macrocycle) would affect the binding of carbon monoxide by electrogenerated $(TPPBr_x)Fe^{II}$ and $[(TPPBr_x)Fe^{II}Cl]^-$. Both of these points are investigated in the present study.

Experimental Section

Chemicals. Benzonitrile (PhCN) was purchased from Aldrich Chemical Co. and distilled over P_2O_5 under vacuum prior to use. Absolute dichloromethane (CH_2Cl_2) over molecular sieves was obtained from Fluka Chemical Co. and used without further purification. Tetrahydrofuran (THF) from EM Science was used without further treatment. Tetra-*n*-butylammonium perchlorate (TBAP), from Sigma Chemical Co., was recrystallized from ethyl alcohol and dried under vacuum at 40 °C for at least 1 week prior to use. Silver perchlorate (99.9%), $AgClO_4 \cdot H_2O$, packed under argon, from Johnson Matthey Electronics was used as received. Sodium borohydride, from Spectrum Chemical MFG Corp., was used without further purification. All other reagents were of analytical grade, purchased from Carlo Erba or Aldrich, and were used without further purification unless otherwise indicated. Carbon monoxide was purchased from Matheson Co.

Table 1. FAB Mass Spectral and UV−Vis Data for $(TPPBr_x)FeCl$ (x = 1−8)

compound	*m/z* found	*m/z* calcd	λ_{max}[a] (nm)		
$(TPPBr_1)FeCl$	746.2	747.5	383 (sh)	418	512
$(TPPBr_2)FeCl$	826.2	826.4	386 (sh)	422	514
$(TPPBr_3)FeCl$	906.2	905.3	375 (sh)	428	516
$(TPPBr_4)FeCl$	984.5	984.2	385 (sh)	432	520
$(TPPBr_5)FeCl$	1062.3	1063.1	390 (sh)	432	520
$(TPPBr_6)FeCl$	1140.5	1141.9	406 (sh)	448	526
$(TPPBr_7)FeCl$	1221.6	1220.8	410 (sh)	452	530
$(TPPBr_8)FeCl$	1300.4	1299.7	418 (sh)	460	536

[a] In CH_2Cl_2.

Synthesis. $(TPP)H_2$ and (TPP)Zn were synthesized according to literature procedures.[36] *N*-Bromosuccinimide was purified as reported in the literature.[37]

$(TPPBr_x)H_2$ Where $x = 1-4$ and 6−8. $(TPPBr_1)H_2$, $(TPPBr_2)H_2$, $(TPPBr_3)H_2$, $(TPPBr_4)H_2$, $(TPPBr_6)H_2$, $(TPPBr_7)H_2$, and $(TPPBr_8)H_2$ were synthesized as reported in the literature.[25,38]

$(TPPBr_5)H_2$. (TPP)Zn (677 mg, 1 mmol) was dissolved in 250 mL of dry (P_2O_5) CCl_4, and *N*-bromosuccinimide (1246 mg, 7 mmol) was added to the solution, which was then refluxed for 4 h in air and protected from moisture with a $CaCl_2$ valve. The solvent was evaporated and the residue chromatographed on Al_2O_3. The first green fraction was collected, the solvent evaporated, and the residue dissolved in 200 mL of CH_2Cl_2. Trifluoroacetic acid (3 mL) was added and the solution stirred under nitrogen for 4 h, after which it was washed first with water and then with saturated $NaHCO_3$. Evaporation of the solvent gave a residue that was chromatographed on a silica gel column, using $CHCl_3$/*n*-hexane (1:1) as eluent. The second eluted fraction was collected, evaporated, and recrystallized from $CHCl_3$/*n*-hexane (1:3) to give 200.3 mg of the final product. Total yield: 20.1%. ^{1}H NMR ($CDCl_3$, 400 MHz): δ (ppm) = 8.4−8.8 (multiplet, 3H, pyr), 8.05−8.2 (multiplet, 8H, *o*-H_{phenyl}), 7.65−7.85 (multiplet, 12H, *m*-H_{phenyl} and *p*-H_{phenyl}). MS (FAB/NBA): m/z 1007.5 $[M - 2H]^+$. UV−vis ($CHCl_3$): λ_{max} (nm) = 440, 536, 687. Anal. Calcd for $C_{44}H_{25}N_4Br_5$: C, 52.37; H, 2.50; N, 5.55. Found: C, 53.01; H, 2.65; N, 5.76.

$(TPPBr_1)FeCl$ and $(TPPBr_2)FeCl$. The mono- and dibrominated iron derivatives were obtained as reported in the literature.[36] In a typical preparation, 100 mg of $(TPPBr_1)H_2$ or $(TPPBr_2)H_2$ was dissolved in 50 mL of acetic acid, 1 mL of pyridine. $FeSO_4 \cdot 7H_2O$ (saturated aqueous solution) was added (1 mL), and the resulting solution was degassed for 10 min under nitrogen and then kept at 60 °C for 1 h under continued bubbling. Evaporation of the solvent under vacuum gave a residue that was purified on a silica gel column eluting with $CHCl_3$. The second eluted fraction was washed with a 5% HCl solution and dried on NaCl after which it was recrystallized from CH_2Cl_2/*n*-hexane (1:2) to give the desired compounds in yields of 50% for $(TPPBr_1)FeCl$ and 60% for $(TPPBr_2)FeCl$. Mass spectral, UV−vis, and elemental analysis data are given in Tables 1 and 2.

$(TPPBr_x)FeCl$ Where $x = 3-8$. The Fe(III) porphyrins with three to eight Br groups were synthesized and purified according to the metal carbonyl method reported by Groves and Myers.[39] In a typical preparation, 100 mg of $(TPPBr_x)H_2$ was dissolved in 25 mL of dry

(27) Hammouche, M.; Lexa, D.; Momenteau, M.; Saveant, J.-M. *J. Am. Chem. Soc.* **1991**, *113*, 8455.
(28) Barkigia, K. M.; Chantranupong, L.; Smith, K. M.; Fajer, J. *J. Am. Chem. Soc.* **1988**, *110*, 7566.
(29) (a) Barkigia, K. M.; Renner, M. W.; Furenlid, L. R.; Medforth, C. J.; Smith, K. M.; Fajer, J. *J. Am. Chem. Soc.* **1993**, *115*, 3627. (b) Ghosh, A. *J. Am. Chem. Soc.* **1995**, *117*, 4631.
(30) Kadish, K. M.; Van Caemelbecke, E.; D'Souza, F.; Medforth, C. J.; Smith, K. M.; Tabard, A.; Guilard, R. *Inorg. Chem.* **1995**, *34*, 2984.
(31) Sparks, L. D.; Medforth, C. J.; Park, M. S.; Chamberlain, J. R.; Ondrias, M. R.; Senge, M. O.; Smith, K. M.; Shelnutt, J. A. *J. Am. Chem. Soc.* **1993**, *115*, 581.
(32) Renner, M. W.; Barkigia, K. M.; Zhang, Y.; Medforth, C. J.; Smith, K. M.; Fajer, J. *J. Am. Chem. Soc.* **1994**, *116*, 8582.
(33) Brigaud, O.; Battioni, P.; Mansuy, D. *New. J. Chem.* **1992**, *16*, 1031.
(34) Hodge, J. A.; Hill, M. G.; Gray, H. B. *Inorg. Chem.* **1995**, *34*, 809.
(35) Kadish, K. M.; Morrison, M. M.; Constant, L. A.; Dickens, L.; Davis, D. G. *J. Am. Chem. Soc.* **1976**, *98*, 8387.
(36) Fuhrhop, J. H.; Smith, K. M. *Porphyrins and Metalloporphyrins*; Elsevier Scientific Publishing Co.: Amsterdam, 1975; Section H, p 757.
(37) Perrin, D. D.; Armarego, W. L. F. *Purification of Laboratory Chemicals*, 3rd ed.; Pergamon Press: New York, 1988; p 105.
(38) Callot, H. J. *Bull. Soc. Chim. Fr.* **1974**, *7*−8, 1492.
(39) Groves, J. T.; Myers, R. S. *J. Am. Chem. Soc.* **1983**, *105*, 5791.

Table 2. Elemental Analyses of ($TPPBr_x$)FeCl Complexes (x = 1−8)

	% C		% H		% N	
compound	calcd	found	calcd	found	calcd	found
($TPPBr_1$)FeCl	67.50	67.58	3.48	3.53	7.16	7.02
($TPPBr_2$)FeCl	61.32	60.95	3.04	2.99	6.50	6.03
($TPPBr_3$)FeCl	56.18	55.98	2.68	2.58	5.96	5.99
($TPPBr_4$)FeCl	51.83	52.02	2.37	2.47	5.49	5.60
($TPPBr_5$)FeCl	48.11	47.60	2.11	2.02	5.10	5.25
($TPPBr_6$)FeCl	44.89	45.02	1.88	1.90	4.76	4.99
($TPPBr_7$)FeCl	42.07	42.77	1.68	1.86	4.46	4.06
($TPPBr_8$)FeCl	39.58	38.92	1.51	1.79	4.20	3.99

(Na), argon-degassed toluene. $Fe(CO)_5$ (0.1 mL) and I_2 (10 mg) were added, and the solution was kept at 60 °C for 2 h under argon. The solvent was evaporated under vacuum and the residue chromatographed on alumina, eluting with chloroform. The second fraction was collected, washed with 5% HCl, and dried on NaCl. Evaporation of the solvent and recrystallization from CH_2Cl_2/*n*-hexane (1:3) led to the final product in yields of 70−80%. Mass spectral, UV−vis, and elemental analysis data are given in Tables 1 and 2.

Instrumentation. Cyclic voltammetry was carried out with an EG&G Model 173 potentiostat or an IBM Model EC 225 voltammetric analyzer. Current−voltage curves were recorded on an EG&G Princeton Applied Research Model RE-0151 X-Y recorder. A three-electrode system was used, consisting of a glassy carbon or platinum button working electrode, a platinum wire counter electrode, and a saturated calomel reference electrode (SCE). This reference electrode was separated from the bulk of the solution by a fritted-glass bridge filled with the solvent/supporting electrolyte mixture. All potentials are referenced to SCE.

Mass spectra were obtained on a VG-4 mass spectrometer using *m*-nitrobenzyl alcohol or 2-aminoglycerol as the matrix. ^{1}H NMR spectra were recorded in $CDCl_3$ on a Bruker AM-400 spectrophotometer using TMS as internal standard. UV−vis spectra were obtained with a HP-8452A spectrophotometer. Elemental analyses were performed by the Analytical Laboratory of the University of Padova, Italy.

UV−visible spectroelectrochemical experiments were performed with an optically transparent platinum thin-layer electrode of the type described in the literature.[40] Potentials for oxidation or reduction of each compound were applied with an EG&G Model 173 potentiostat. Time-resolved UV−visible spectra were recorded with either a Tracor Northern Model 6500 rapid scan spectrophotometer/multichannel analyzer or a Princeton Instrument PDA-1024 diode array rapid scanning spectrophotometer.

Infrared spectroelectrochemical measurements were made with an FTIR Nicolet Magna-IR 550 spectrometer using a specially constructed light-transparent three-electrode cell.[41] The background was obtained by recording the IR spectrum of ($TPPBr_x$)FeCl in CH_2Cl_2 under a CO atmosphere without any applied potential. The IR spectrum of the electroreduced compound under CO was taken after bubbling CO through the spectroelectrochemical cell for 5−15 min prior to applying a potential, and a blanket of CO was maintained above the solution during the measurement.

EPR spectra were recorded at 77 K using a Bruker ESP 380 E spectrometer. The g values were measured with respect to diphenylpicrylhydrazyl ($g = 2.0036 \pm 0.0003$).

Results and Discussion

Cyclic voltammograms of representative ($TPPBr_x$)FeCl complexes in PhCN, 0.1 M TBAP are presented in Figure 1, and the redox potentials for each electrochemical process are summarized in Table 3. Each compound undergoes two oxidations and either three or four reductions within the anodic or cathodic potential limits of the solvent.

Electrooxidation of ($TPPBr_x$)FeCl. The two oxidations of ($TPPBr_x$)FeCl (processes IV and V) are reversible to quasireversible for all of the studied compounds. (TPP)FeCl undergoes two one-electron oxidations, leading to an iron(III) π cation radical and dication;[26] this also appears to be the case for each ($TPPBr_x$)FeCl complex on the basis of comparisons between the UV−visible spectra of the singly and doubly oxidized compounds and spectra obtained after the same electrode reactions of (TPP)FeCl. Examples of the resulting reversible spectral changes are shown in Figure 2 for the case of ($TPPBr_2$)FeCl, while Table 4 summarizes the UV−vis data for neutral and electrooxidized ($TPPBr_x$)FeCl where x = 0, 2, 4, and 7. For all four compounds, the Soret band decreases in intensity upon oxidation and exhibits a blue shift of 1−14 nm depending upon the number of Br groups on the macrocycle.

The values of $E_{1/2}$ for the two oxidations are plotted vs the number of Br groups in Figure 3a, while Figure 3b shows the correlation involving $\Delta E_{1/2}$ between processes IV and V and the number of Br groups on ($TPPBr_x$)FeCl. The first oxidation of ($TTPBr_x$)FeCl shifts positively in potential upon going from $x = 0$ to $x = 2$ but negatively upon going from $x = 3$ to $x = 8$. An opposite trend is seen for the second oxidation; i.e., a negative shift is seen upon going from $x = 0$ to 2 and a positive one from $x = 3$ to 8. Thus, the absolute potential difference between the two oxidations ($\Delta E_{1/2}$) varies with the number of Br groups on the macrocycle and increases linearly from 230 mV in the case of ($TPPBr_2$)FeCl to 450 mV in the case of

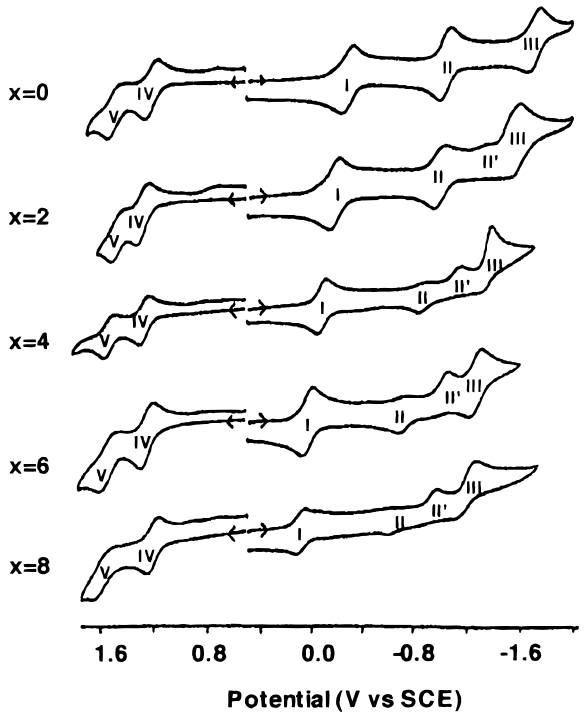

Figure 1. Cyclic voltammograms of representative ($TPPBr_x$)FeCl complexes (x = 0, 2, 4, 6, 8) in PhCN, 0.1 M TBAP. Scan rate = 0.1 V/s.

Table 3. Half-Wave Potentials (V vs SCE) for Reduction and Oxidation of ($TPPBr_x$)FeCl, in PhCN Containing 0.1 M TBAP[a]

	oxidation		reduction			
compound	V	IV	I	II	II′	III
(TPP)FeCl	1.52	1.20	−0.29	−1.06		−1.73
($TPPBr_1$)FeCl	1.52	1.24	−0.26	−1.07		−1.73
($TPPBr_2$)FeCl	1.51	1.28	−0.18	−1.01		−1.61
($TPPBr_3$)FeCl	1.53	1.27	−0.13	−0.97	−1.26	−1.60
($TPPBr_4$)FeCl	1.56	1.26	−0.07	−0.86	−1.18	−1.37
($TPPBr_5$)FeCl	1.58	1.26	−0.02	−0.83	−1.14	−1.36
($TPPBr_6$)FeCl	1.60	1.24	0.04	−0.73	−1.17[b]	−1.28
($TPPBr_7$)FeCl	1.62	1.21	0.06	−0.67	−1.13[b]	−1.24
($TPPBr_8$)FeCl	1.64	1.19	0.10	−0.62	−0.97[b]	−1.20

[a] Identification of processes I−V are given in Figure 1. [b] E_{pc} at 0.1 V/s.

(40) Lin, X. Q.; Kadish, K. M. *Anal. Chem.* **1985**, *57*, 1498.
(41) Lin, X. Q.; Mu, X. H.; Kadish, K. M. *Electroanalysis* **1989**, *1*, 35.

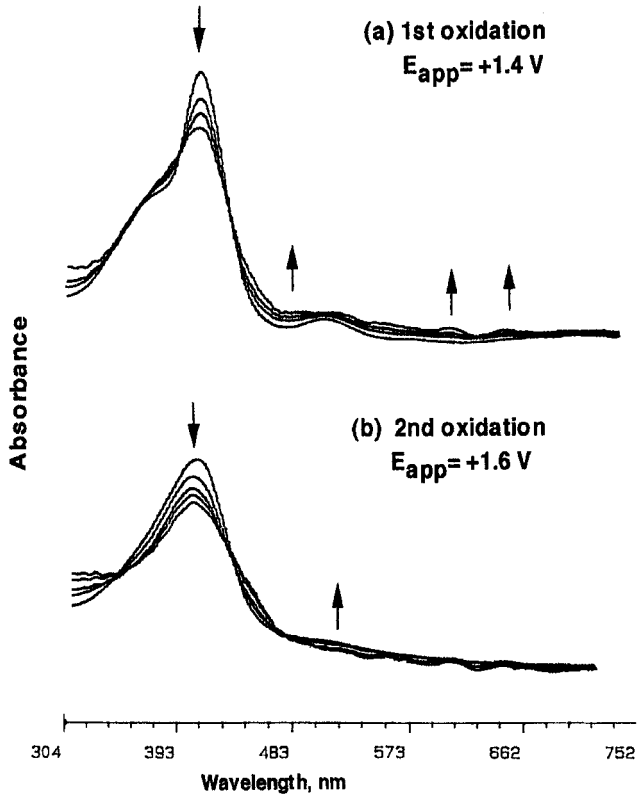

Figure 2. Time-resolved thin-layer electronic absorption spectra of (TPPBr$_2$)FeCl in PhCN, 0.2 M TBAP upon stepping the potential from (a) 0.0 to +1.4 V and (b) +1.4 to +1.6 V.

Table 4. Absorption Maxima (λ, nm) and Corresponding Molar Absorptivities ($10^{-3}\epsilon$) for the Soret Band of (TPPBr$_x$)FeCl (x = 0, 2, 4, 7) and Their Electrogenerated Products in PhCN, 0.2 M TBAP

	electrode reactions			
compound	process IV	none	process I	process II (or II′)[a]
(TPP)FeCl	412 (76)	411 (95)	424 (131)	427 (83)
(TPPBr$_2$)FeCl	417 (76)	421 (92)	438 (129)	439 (81)
(TPPBr$_4$)FeCl	422 (56)	425 (96)	441 (145)	446 (77)
(TPPBr$_7$)FeCl	441 (130)	455 (180)	477 (290)	473 (140)

[a] II′ for (TPPBr$_x$)FeCl with x = 6−8.

(TPPBr$_8$)FeCl. Interestingly, the latter value is virtually identical to $\Delta E_{1/2}$ between the two ring-centered oxidations of (OETPP)FeCl[30] (460 mV) and (DPP)FeCl[42] (460 mV) (DPP = the dianion of dodecaphenylporphyrin), two molecules that possess a severely distorted macrocycle.[31,42−45]

The oxidative behavior of (TPPBr$_8$)FeCl, (OETPP)FeCl, and (DPP)FeCl contrasts significantly with data for other highly distorted porphyrins such as (TFPPBr$_8$)Zn[34] and [(TPPBr$_x$)Co^{III}]$^{+}$ [25] (x = 6−8). The latter two series of compounds undergo two ring-centered one-electron oxidations, both of which are overlapped in potential to give a global two-electron transfer. It was suggested[34] that the electrogenerated [(TFPPBr$_8$)Zn]$^+$ π cation radical is kinetically unstable and that this instability was related to two factors which influence the relative energies of the a and b$_1$ orbitals. One factor was the presence

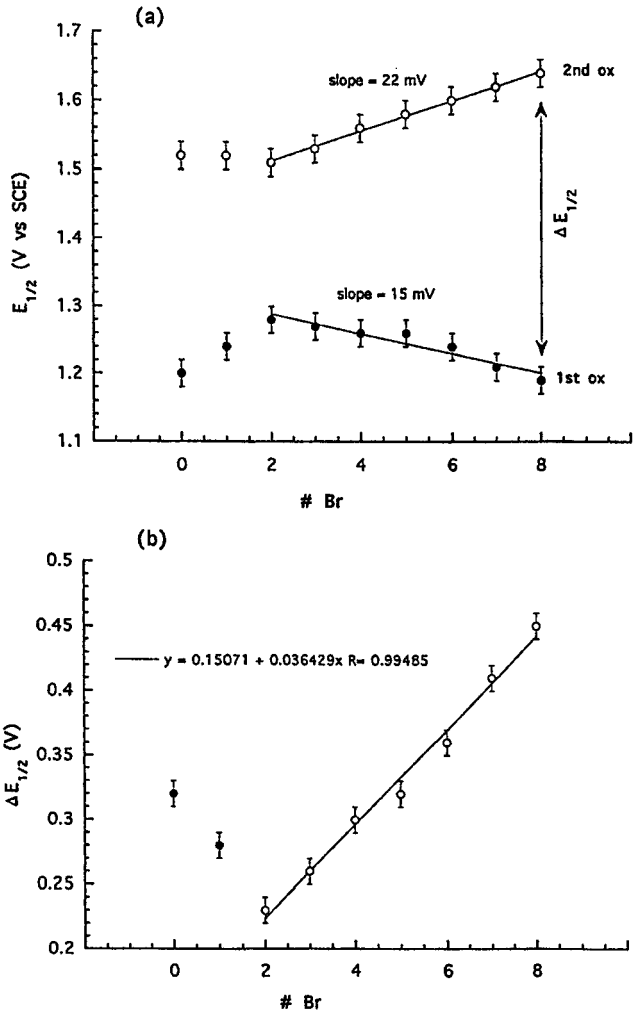

Figure 3. Plots of (a) $E_{1/2}$ vs the number of Br groups for the first and second oxidations of (TPPBr$_x$)FeCl and (b) $\Delta E_{1/2}$ between the first and second oxidations of (TPPBr$_x$)FeCl vs the number of Br groups.

of electron-withdrawing substituents at the meso positions of the porphyrin ring and the other a distortion of the porphyrin macrocycle.

In summary, $\Delta E_{1/2}$ between the two ring-centered oxidations of porphyrins may *increase* or *decrease* with increased nonplanarity of the molecule, but the exact effect seems to depend upon the type of central metal ion and/or its ligand environment. For example, $\Delta E_{1/2}$ between the two ring-centered oxidations of (TPPBr$_8$)FeCl (450 mV) is *larger* than $\Delta E_{1/2}$ between the two ring-centered oxidations of (TPP)FeCl (320 mV). This contrasts with the case of cobalt porphyrins having the same TPPBr$_x$ macrocycles, where $\Delta E_{1/2}$ between the two ring-centered oxidations of [(TPPBr$_8$)Co]$^+$ (70 mV) is *smaller* than $\Delta E_{1/2}$ between the two ring-centered oxidations of [(TPP)Co]$^+$ (190 mV).[24]

Resonance Raman[31,46−48] and structural studies[49] have revealed that an S_4-ruffling of the porphyrin core is characterized by a shortening of the M−N$_p$ bonds (M is a given metal and N$_p$ a ring nitrogen), and this could also lead to an increased overlap between the π ring and metal d orbitals depending upon the type of central metal ion and/or the M−N$_p$ bond lengths. The ionic radii[50] of Fe(III) (0.64 Å) and Co(III) (0.63 Å) are

(42) Simpson, M. C.; Showalter, M.; J., M.; Jentzen, W.; Hobbs, J. D.; Medforth, C. J.; Nurco, D. J.; Forsyth, T. P.; Smith, K. M.; D'Souza, F.; Van Caemelbecke, E.; Kadish, K. M.; Shelnutt, J. A. Manuscript in preparation.
(43) Ochsenbein, P.; Ayougou, K.; Mandon, D.; Fisher, J.; Weiss, R.; Austin, R. N.; Jayaraj, K.; Gold, A.; Terner, J.; Fajer, J. *Angew. Chem., Int. Ed. Engl.* **1994**, *33*, 348.
(44) Medforth, C. J.; Smith, K. M. *Tetrahedron. Lett.* **1990**, *31*, 5583.
(45) Mandon, D.; Ochsenbein, P.; Fischer, J.; Weiss, R.; Jayaraj, K.; Austin, R. N.; Gold, A.; White, P. S.; Brigaud, O.; Battioni, P.; Mansuy, D. *Inorg. Chem.* **1992**, *31*, 2044.
(46) Choi, S.; Spiro, T. G.; Langry, K. C.; Smith, K. M.; Budd, L. D.; La Mar, G. N. *J. Am. Chem. Soc.* **1982**, *104*, 4345.
(47) Spiro, T. G. *Iron Porphyrins, Part 2*; Addison-Wesley: Reading MA, 1983, p 89.
(48) Piffat, C.; Melamed, D.; Spiro, T. G. *J. Phys. Chem.* **1993**, *97*, 7441.
(49) Scheidt, W. R.; Reed, C. A. *Chem. Rev.* **1981**, *81*, 543.

almost identical, suggesting that the size of the metal ion may not be the most important factor to account for the difference in $\Delta E_{1/2}$ between the two ring-centered oxidations of $(TPPBr_8)$-FeCl and $[(TPPBr_8)Co^{III}]^+$.

The average of the $M-N_p$ bond lengths in $(TPPBr_8)FeCl$ should be higher than that in the singly oxidized product of $(TPPBr_8)Co$ which, in PhCN, 0.1 M TBAP, most likely exists as the bis-PhCN complex, $[(TPPBr_8)Co^{III}(PhCN)_2]^+$. This is the case for highly distorted[51] $[(OETPP)Co^{III}(py)_2]^+$, which has an average $M-N_p$ bond length of 1.931 Å as compared to 1.971 Å for (OETPP)FeCl.[31] It should also be noted that (OETPP)-Cu, which has an average $M-N_p$ bond length of 1.977 Å[31], shows a 460 mV potential separation between its two ring-centered oxidations in butyronitrile,[32] and this value is similar to the 450 mV potential separation between the two ring-centered oxidations of $(TPPBr_8)FeCl$ in PhCN.

Finally it can be pointed out that $\Delta E_{1/2}$ between the two ring-centered oxidations of $(TPPBr_x)FeCl$ in CH_2Cl_2 is similar to $\Delta E_{1/2}$ in PhCN, thus implying that the solvation of the oxidized porphyrin, i.e. $[(TPPBr_x)FeCl)]^+$, is not the main factor contributing to the correlation between $\Delta E_{1/2}$ and the number of Br groups on the macrocycle (see Figure 3b). The present data rather suggest that the $M-N_p$ bond lengths, which influence the overlap between the π ring and metal d orbitals, may play a key role in determining the potential separation between the two ring-centered oxidations of nonplanar porphyrins.

Electroreduction of $(TPPBr_x)FeCl$. Each $(TPPBr_x)FeCl$ complex undergoes up to four reductions by cyclic voltammetry in PhCN. The first, labeled as process I in Figure 1, is reversible in all cases and involves a conversion of Fe(III) to Fe(II).[24] The second, labeled as process II, is reversible only for compounds with $x = 0$ or 1. As the number of Br groups increases above 2, the cathodic peak current intensity of process II becomes smaller than that of process I while a new irreversible reduction peak, labeled as process II′ in Figure 1, appears at a potential which is 290−460 mV more negative than the $E_{1/2}$ of process II (see Table 3 for exact potentials). Process II′ is coupled to the anodic peak of process II as seen in Figure 1.

Kadish and Rhodes[52] have shown that the first reduction of (TPP)FeCl in PhCN results in a mixture of $[(TPP)Fe^{II}Cl]^-$ and $(TPP)Fe^{II}$. Similar equilibria between halide-bound and halide-free Fe(II) forms of the porphyrin also exist after the first reduction of $(TPPBr_x)FeCl$, and this was confirmed by cyclic voltammograms of the compounds in PhCN solutions with and without added $AgClO_4$. For example, the addition of $AgClO_4$ to a PhCN solution containing $(TPPBr_8)FeCl$ leads to precipitation of AgCl and the subsequent formation of $(TPPBr_8)FeClO_4$, a compound which is reduced at $E_{1/2} = +0.49$ V. The latter process, labeled as I′ in Figure 4, is located at a potential that is 390 mV more positive than $E_{1/2}$ for the Fe(III)/Fe(II) reaction of $(TPPBr_8)FeCl$. Thus, by analogy to $(TPP)FeClO_4$ and (TPP)-FeCl,[26] process I′ is assigned to a conversion of $(TPPBr_8)FeClO_4$ to $(TPPBr_8)Fe^{II}$.

Process II′ almost completely disappears after addition of 3.0 equiv of $AgClO_4$ to the solution, and the Fe(II) reduction occurs mainly *via* process II, as shown in Figure 4. This process is assigned as a reduction of $(TPPBr_x)Fe^{II}$ to $[TPPBr_x)Fe]^-$, while process II′ is proposed to involve a reduction of $[(TPPBr_x)Fe^{II}Cl]^-$ to $[(TPPBr_x)Fe]^-$. This is also the conclusion which results from analysis of the UV−vis spectroelectrochemical data (see following section). Finally, $E_{1/2}$ of process III remains unchanged after addition of 1.0−3.0 equiv of $AgClO_4$ to solutions of $(TPPBr_8)FeCl$, and this is consistent with the fact that the Cl^- axial ligand is not coordinated to doubly reduced $(TPPBr_8)$-FeCl.

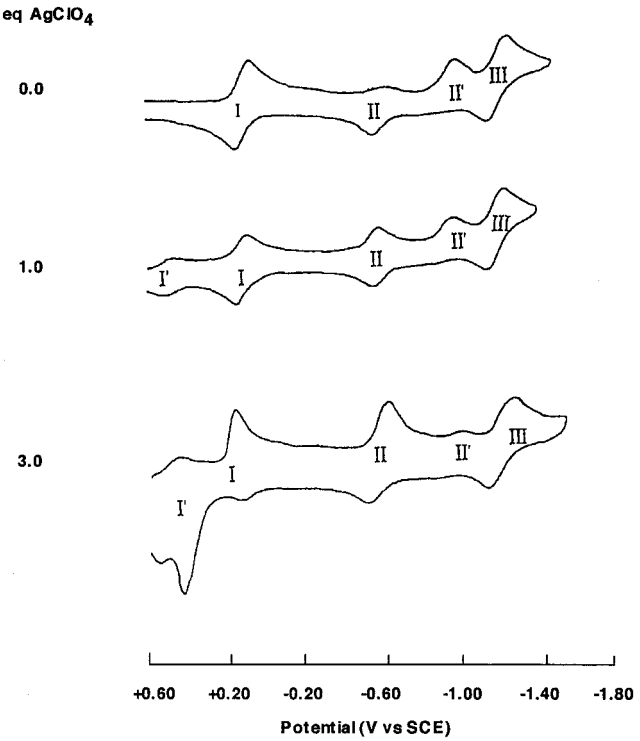

Figure 4. Cyclic voltammograms of 0.8×10^{-3} M $(TPPBr_8)FeCl$ in PhCN, 0.1 M TBAP containing 0.0, 1.0, and 3.0 equiv of $AgClO_4$.

The solution equilibrium which exists between electrogenerated $(TPP)Fe^{II}$ and $[(TPP)Fe^{II}Cl]^-$ is displaced toward the anionic form of the porphyrin by addition of (TBA)Cl to solution, and the resulting complex shows a UV−vis spectrum with only two visible bands.[52] Three bands are observed in the visible region of the Fe(II) complexes having zero to four Br groups, but only two are seen for those complexes with $x > 5$, thus suggesting that $[(TPPBr_x)Fe^{II}Cl]^-$ is the dominant species in solution for compounds with six to eight Br groups. Examples of the UV−vis spectra are shown in Figure 5 for the singly reduced products of $(TPPBr_2)FeCl$ and $(TPPBr_6)FeCl$. The electrogenerated Fe(II) porphyrin with two Br groups has bands at 529, 563, and 605 nm, while the one with six Br groups has visible bands at 591 and 637 nm.

Further reduction of $[(TPPBr_x)Fe^{II}Cl]^-$ *via* process II′ in Figure 1 leads to a loss of the chloride axial ligand, and $[(TPPBr_x)Fe]^-$ is then the only porphyrin present in solution. The UV−visible spectrum of electrogenerated $[(TPPBr_x)Fe]^-$ shows a broad Soret band whose molar absorptivity is smaller than that for the Soret band of the singly-reduced Fe(II) product (see Table 4).

Doubly reduced (TPP)FeCl and $(TPPBr_4)FeCl$ both contain iron(I), as indicated by their ESR spectra,[53] and a similar metal oxidation state is proposed for the other seven $[(TPPBr_x)Fe]^-$ complexes on the basis of data in the literature and results in the present study for $[(TPPBr_7)Fe]^-$. The doubly reduced form of $(TPPBr_7)FeCl$ was generated by chemical reduction of the neutral porphyrin using excess sodium borohydride and its ESR spectrum then recorded in frozen THF. This spectrum is shown in Figure 6 and is characterized by signals at $g = 2.21$ and 1.96. Additional weaker signals are also seen at $g \approx 4.3$ and g

(50) *Handbook of Chemistry and Physics*, 66th ed.; CRC Press, Inc.; Boca Raton, FL, 1985−1986; p F-164.
(51) X-ray crystallographic data for (OETPP)Ni[31] and Ni porphyrins with eight halogens at the pyrrole β positions[46] show that these two types of metallo complexes are severely distorted and have similar $M-N_p$ bond lengths.
(52) Kadish, K. M.; Rhodes, R. K. *Inorg. Chem.* **1983**, *22*, 1090.
(53) Donohoe, R. J.; Atamian, M.; Bocian, D. F. *J. Am. Chem. Soc.* **1987**, *109*, 5593.

Scheme 1

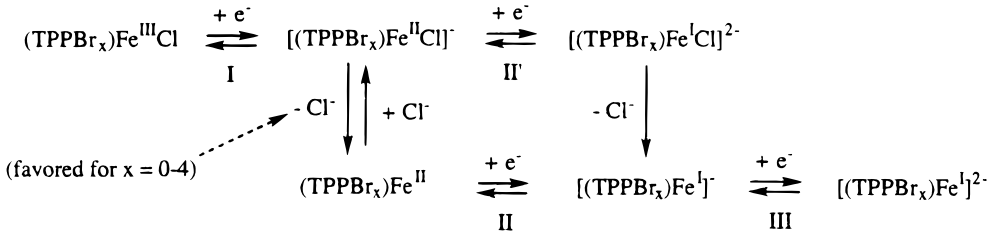

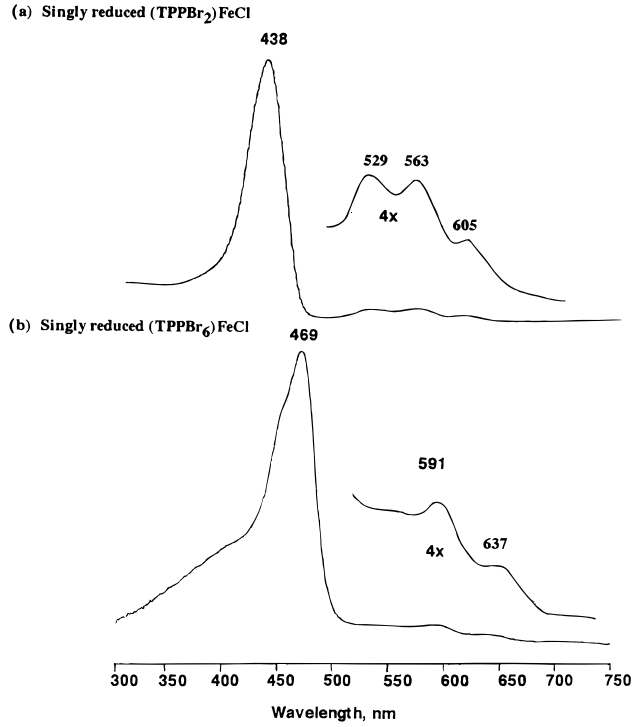

Figure 5. Electronic absorption spectra of singly reduced (a) (TPPBr$_2$)FeCl and (b) (TPPBr$_6$)FeCl in PhCN, 0.2 M TBAP.

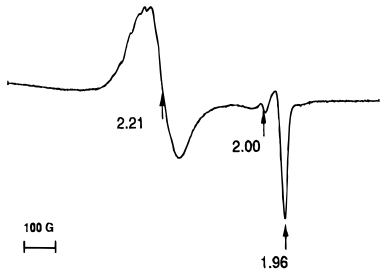

Figure 6. EPR spectrum of [(TPPBr$_7$)Fe^{I}]$^-$ in THF at 77 K.

$\approx$ 2.0 and are assigned to an iron peroxo species produced by reaction of the iron(I) porphyrin with trace oxygen.[54] The ESR spectrum of [(TPPBr$_7$)Fe]$^-$ in frozen THF is similar to the ESR spectrum of [(TPP)Fe]$^-$ which has g values at 2.28 and 1.93 in frozen DMF,[53] thus suggesting that the second reduction product of (TPPBr$_7$)FeCl also contains iron(I).

The third reduction of (TPPBr$_x$)FeCl (labeled as process III in Figure 1) is quasireversible to reversible by cyclic voltammetry. This electrode reaction has been assigned to the conversion of an iron(I) porphyrin to an iron(I) porphyrin π anion radical[55] in the case of (TPP)FeCl. A linear relationship exists between $E_{1/2}$ for process III and the number of Br groups on (TPPBr$_x$)FeCl (figure not shown), and this suggests that all eight iron brominated porphyrins undergo a third reduction at the same site of the molecule.

In summary, the overall electroreduction of (TPPBr$_x$)FeCl in PhCN, 0.1 M TBAP is proposed to occur as shown in Scheme 1.

A dissociation of the chloride axial ligand from [(TPPBr$_x$)Fe^{II}Cl]$^-$ is favored for compounds with zero to four Br groups and occurs rapidly for the compounds with $x = 0$ or 1. The electron density at the iron(III) or iron(II) center of the porphyrin decreases as the number of electron-withdrawing Br groups on the macrocycle is increased, thus resulting in a strengthening of the Fe−Cl bond for the higher brominated compounds. Consequently, the second reduction will occur *via* both processes II and II′ for compounds with $x = 2-5$, conditions under which the relative cyclic voltammetric peak intensities of these processes will depend upon both their potential separation and the degree of ligand dissociation.[26] The [(TPPBr$_x$)Fe^{II}Cl]$^-$ form of the Fe(II) porphyrin which is generated *via* process I is very stable when $x = 6-8$, and a dissociation of the chloride axial ligand in these complexes occurs only after the second reduction and formation of the Fe(I) porphyrin, i.e. after process II′.

CO Binding to Electrogenerated Iron(II) Complexes. It has long been known that Fe(II) porphyrins form both mono and bis-CO adducts in nonaqueous media,[56−60] with the exact stoichiometry of the reaction depending upon the partial pressure of CO and any competitive ligand binding reactions. Little, however, is known with respect to how systematic changes in basicity or distortion of the porphyrin macrocycle might affect the CO binding reactions. These studies were therefore carried out for each singly reduced product of (TPPBr$_x$)FeCl in the nonbonding solvent, CH_2Cl_2. The cyclic voltammograms of the porphyrins in CH_2Cl_2, 0.2 M TBAP are very similar in shape to those obtained in PhCN, and the redox potentials for each electrode reaction are almost identical in both solvents under an N_2 atmosphere.

Figure 7 shows the FTIR difference spectra obtained after the first reduction of 0.7 ± 0.1 mM (TPPBr$_x$)FeCl ($x = 0-8$) in CH_2Cl_2, 0.2 M TBAP under a CO atmosphere. The spectra of the compounds with zero to six Br groups show two bands whose relative intensity depends on the number of Br groups. Under the same solution conditions, the spectrum of (TPPBr$_7$)FeCl shows only a single band and no band at all is seen for the spectrum of (TPPBr$_8$)FeCl.

The bands located between 1962 and 1980 cm^{-1} in Figure 7 arise from the ν_{CO} of a mono-CO adduct while the higher energy bands, located between 2028 and 2043 cm^{-1}, are assigned to the asymmetric stretches of a bis-CO adduct.[57] These assignments are consistent with the fact that the band of the bis-CO adduct first decreases in intensity and then disappears as the porphyrin concentration is increased from 0.7 to 2.0 mM. The

(54) Valentine, J. S.; McCandlish, E. *Frontiers of Biological Energetics, Electrons to Tissues*; Academic Press: New York, 1978; p 936.
(55) Hickman, D. L.; Shirazi, A.; Goff, H. M. *Inorg. Chem.* **1985**, *24*, 563.
(56) Wayland, B. B.; Mehne, L. F.; Swartz, J. *J. Am. Chem. Soc.* **1978**, *100*, 2379.
(57) Strauss, H.; Holm, R. H. *Inorg. Chem.* **1982**, *21*, 863.
(58) Rougee, M.; Brault, D. *Biochem. Biophys. Res. Commun.* **1973**, 1364.
(59) Rougee, M.; Brault, D. *Biochemistry* **1975**, *14*, 4100.
(60) Swistak, C.; Kadish, K. M. *Inorg. Chem.* **1987**, *26*, 405.

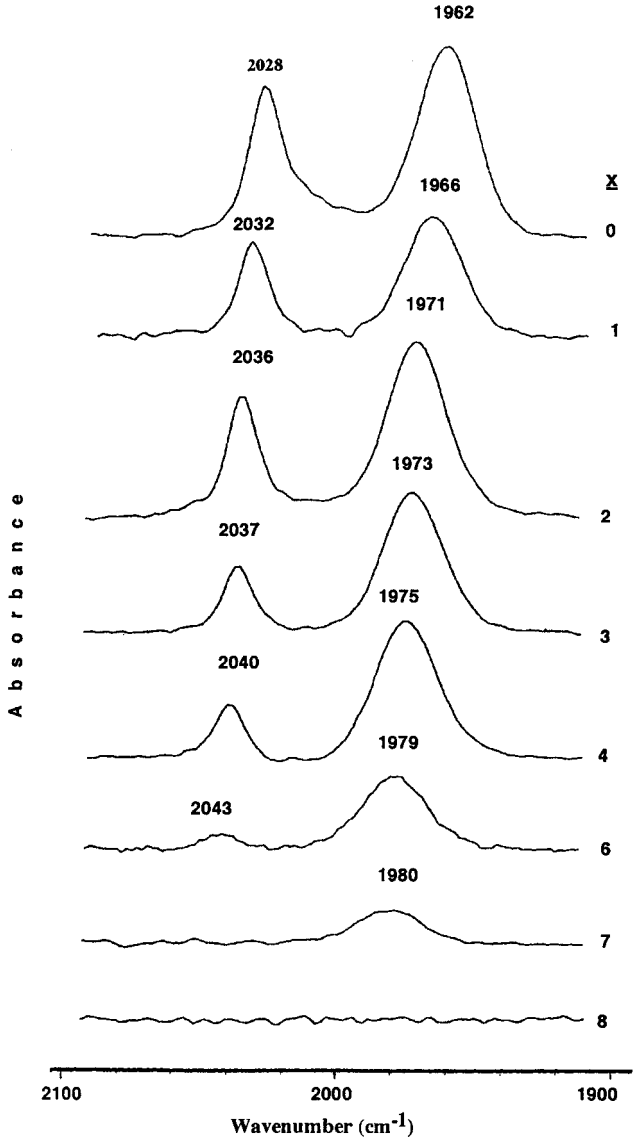

Figure 7. IR spectra of 0.76 mM $(TPPBr_x)FeCl$ ($x = 0-4$ and $6-8$) in CH_2Cl_2, 0.1 M TBAP under a CO atmosphere at a potential slightly more negative than that of process I (see text).

assignments also agree with the expected trans effect of CO, which raises ν_{CO} for the bis-CO adduct as compared to the mono.[56]

The electrochemical and UV−vis spectral data both indicate that the singly reduced products of $(TPPBr_x)FeCl$ are $(TPPBr_x)Fe^{II}$ or $[(TPPBr_x)Fe^{II}Cl]^-$, or a mixture of both, in a nonbinding solvent, with the degree of Cl^- binding to Fe(II) depending upon the overall basicity of the macrocycle. The binding of CO to the Fe(II) forms of $(TPPBr_x)FeCl$ can therefore be interpreted by eqs 1−3.

$$(TPPBr_x)Fe^{II} + CO \rightleftarrows (TPPBr_x)Fe^{II}(CO) \quad (1)$$

$$[(TPPBr_x)Fe^{II}Cl]^- + CO \rightleftarrows [(TPPBr_x)Fe^{II}(CO)Cl]^- \quad (2)$$

$$(TPPBr_x)Fe^{II} + 2CO \rightleftarrows (TPPBr_x)Fe^{II}(CO)_2 \quad (3)$$

Kadish *et al.*[60] have shown that $[(TPP)FeCl]^-$ can be converted to $[(TPP)Fe(CO)Cl]^-$ in CH_2Cl_2, 0.1 M TBACl under a CO atmosphere on the cyclic voltammetry time scale, and our IR spectral data can be interpreted in a similar manner. The 2028 cm^{-1} band, assigned to the ν_{CO} of $(TPP)Fe(CO)_2$, disappears upon going from 0.2 M TBAP to 0.2 M (TBA)Cl while the intensity of the band for the mono-CO adduct remains the same. These data indicate that a bisadduct is not present in solutions containing excess Cl^-, where only the six-coordinate $[(TPPBr_x)Fe(CO)Cl]^-$ species is formed as shown in eq 2.

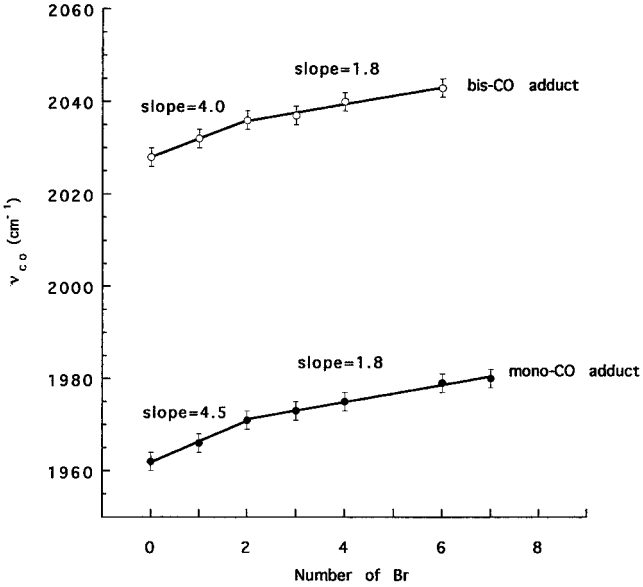

Figure 8. Plots illustrating ν_{CO} of mono- and bisadducts of CO versus the number of Br groups on the porphyrin macrocycle.

Figure 8 illustrates plots of ν_{CO} versus the number of Br groups on the porphyrin macrocycle for both the mono- and bis-adducts. The frequencies of both CO vibrations increase with increase in the number of Br groups on the macrocycle, and this is consistent with a decreased electron density at the Fe(II) center and a weakened Fe−CO bond. As a result, the octabrominated complex does not bind CO at all while the heptabrominated species shows only a weak band at 1980 cm^{-1} (see Figure 7), indicating the presence of a single CO molecule coordinated to the iron(II) form of the porphyrin, which is presumed to exist as $[(TPPBr_7)Fe(CO)Cl]^-$.

Interestingly, ν_{CO} does not show a linear relationship with the number of Br groups on the macrocycle, and this was also the case for $E_{1/2}$ of the first oxidation (see Figure 3a). The fact that similar trends are observed in Figure 3a and Figure 8 suggests that the ring distortion, which arises from an increase in the number of Br groups on the porphyrin macrocycle, stabilizes the Fe−CO bond in both the mono- and bis-CO adducts. The change in ν_{CO} per added Br group is small, but there is no doubt that two correlations exist, one for compounds with $x = 0-2$ and the other for compounds with $x = 3-7$ (or 8). This point is noteworthy, and to our knowledge is the first report where the axial ligand binding affinity of a nonplanar porphyrin for a small molecule, such as CO, will be affected by the nonplanarity of the macrocycle.

Finally, our results have shown that the metal ion and its environment seem to influence the potential separation between the ring-centered oxidations of nonplanar porphyrins. Theoretical and experimental studies with different metal ions should therefore be undertaken in order to better understand this relationship.

Acknowledgment. The support of the Robert A. Welch Foundation (K.M.K.; Grant E-680), The University of Houston Energy Laboratory (K.M.K.) and the Italian MURST (P.T.), and the CNR (P.T.) is gratefully acknowledged. We also thank Giuseppe D'Arcangelo and Fabio Bertocchi for mass spectral and NMR measurements and Dr. T. Wasowicz for ESR measurements.

IC960148C